

---

# Parameter Norm Growth During Training of Transformers

---

William Merrill<sup>ae</sup> Vivek Ramanujan<sup>j</sup> Yoav Goldberg<sup>ae,b</sup> Roy Schwartz<sup>h</sup> Noah Smith<sup>ae,j</sup>

<sup>ae</sup>Allen Institute for AI <sup>j</sup>University of Washington

<sup>b</sup>Bar Ilan University <sup>h</sup>Hebrew University of Jerusalem

## Abstract

The capacity of neural networks like the widely adopted transformer is known to be very high. Evidence is emerging that they learn successfully due to inductive bias in the training routine, typically some variant of gradient descent (GD). To better understand this bias, we study the tendency of transformer parameters to grow in magnitude during training. We find, both theoretically and empirically, that, in certain contexts, GD increases the parameter  $L_2$  norm up to a threshold that itself increases with training-set accuracy. This means increasing training accuracy over time enables the norm to increase. Empirically, we show that the norm grows continuously over pretraining for T5 (Raffel et al., 2019). We show that pretrained T5 approximates a semi-discretized network with saturated activation functions. Such “saturated” networks are known to have a reduced capacity compared to the original network family that can be described in automata-theoretic terms. This suggests saturation is a new characterization of an inductive bias implicit in GD that is of particular interest for NLP. While our experiments focus on transformers, our theoretical analysis extends to other architectures with similar formal properties, such as feedforward ReLU networks.

## 1 Introduction

Modern neural network architectures achieve good generalization performance across many different tasks and application domains. In order for these highly overparameterized models to generalize well, there ought to be some implicit inductive bias or capacity control in the learning algorithms for these models, but it is an interesting open question what this is, or even how to characterize it. In particular, in NLP, transformers (Vaswani et al., 2017) like BERT (Devlin et al., 2019), XLNet (Yang et al., 2019), RoBERTa (Liu et al., 2019), and T5 (Raffel et al., 2019) have pushed the state of the art on an impressive array of NLP tasks. Because these models are so large, their success is tied to the question of how capacity is restricted during training—what prevents transformers from overfitting, allowing the pretrained representation to generalize well to other problems?

A simple case where deep learning theory has studied the generalization properties of gradient descent (GD) is matrix factorization (Gunasekar et al., 2017; Arora et al., 2019; Razin and Cohen, 2020). It has been observed that deep matrix factorization leads to low-rank matrix solutions. Razin and Cohen (2020) argued theoretically that this bias of GD cannot be explained as an implicit regularizer minimizing some norm. Rather, they construct cases where all parameter norms diverge as GD approaches its solution.

Similar ideas have emerged in recent works studying feedforward networks. Analyzing biasless ReLU networks with cross-entropy loss, Poggio et al. (2019, 2020) show that the *magnitude* of the parameter vector continues to increase during GD, whereas its *direction* converges. Li and Arora (2019) present a similar argument for any network that is “scale-invariant”, meaning that scaling the parameters by a constant does not change the output. This property leads the norm to continuously increase

during training. The perspective developed by such works challenges the conventional wisdom that GD reaches a local minimum during training. Rather, it suggests that GD follows a norm-increasing *trajectory* along which network behavior stabilizes. These analyses motivate investigation of this trajectory-driven perspective of training.

From a statistical perspective, work in this vein has considered the implications of these training dynamics for margin maximization (Poggio et al., 2019; Nacson et al., 2019; Lyu and Li, 2019). While these works vary in the specific architectures they consider and assumptions they make, they reach similar conclusions: GD finds trajectories leading to infinite-norm solutions that maximize the margin. As a max-margin solution has a simple decision boundary, it should generalize better than an arbitrary solution achieving low training loss. Thus, this point of view partially explains why growing norm is associated with better generalization performance.

But growing norm has another interpretation for NLP models. Past work characterizes the capacity of networks with infinitely scaled norm in terms of formal language and automata theory. Merrill (2019) and Merrill et al. (2020) propose *saturated networks*, an abstraction to allow for a theoretical analysis of the capacity of NLP architectures. A network is analyzed by assuming it “saturates” its nonlinearities, which means replacing functions like  $\sigma$  and  $\tanh$  with step functions. This is equivalent to uniformly scaling the weights by a constant approaching  $\infty$ . Saturation reduces complex connectionist NLP models to discrete computational models resembling automata, making some kinds of theoretical analysis easier. For many common architectures, the saturated capacity is known to be significantly weaker than the full capacity of the network with rational-valued weights (Merrill, 2019), which, classically, is Turing-complete for even simple RNNs (Siegelmann and Sontag, 1992).

For example, it is possible to hand-construct a stack-like data structure for an RNN or LSTM (Kirov and Frank, 2012). However, a saturated LSTM does not have the computational capacity to simulate a stack (Merrill, 2019). Rather, saturated LSTMs resemble classical counter machines (Merrill, 2019), a model of computation limited in its ability to model hierarchical structure. Experimental findings suggest that LSTMs trained on synthetic tasks learn counter-like representations (Weiss et al., 2018; Suzgun et al., 2019a), and that they fail on tasks requiring stacks and other deeper models of structure (Suzgun et al., 2019b). Similarly, Shibata et al. (2020) found that LSTM language models trained on natural language data acquire representations approximating counters.

Recent work has extended saturation analysis to transformers (Hahn, 2020; Merrill, 2019; Merrill et al., 2020). The saturated transformer reduces to an “arg max” hard attention machine where attention focuses on the values with maximum key-query similarity. In this case of ties, attention is distributed uniformly over all values with maximal similarity. While the capacity of this machine is not fully understood, it can implement a weak counting mechanism similar to the LSTM. Bhattamishra et al. (2020) show that transformers can learn counting tasks using this construction, and that they struggle on tasks requiring more complicated structural representations. Thus, experiments have shown that the synthetic tasks LSTMs or transformers can learn is predicted by their saturated counterparts. Thus, Merrill et al. (2020) conjecture that the saturated capacity might represent a class of behaviors implicitly learnable by GD, although it is unclear why this should be the case.

In this work, we take the perspective that thoroughly understanding the dynamics of training—in particular, norm growth—might clarify the biases or capacity restrictions imposed by GD. We study the norm growth phenomenon in transformers, both empirically and theoretically. We prove that, with some light assumptions, any network where the parameter norm diverges during training approaches a saturated network. Further, in certain contexts, we find there is a link between training accuracy and norm growth, with the norm growing more for models that achieve better performance on the train set. We show this theoretically in a simplified formal model, and then empirically for various components of the transformer model. Using historical training checkpoints, we then verify that the norm increased continuously over the training of the large transformer model T5 (Raffel et al., 2019). Finally, we consider the effect of norm growth on the behavior of the model. Theoretically, transformers increasingly approximate saturated networks as their norm grows. Empirically, we find that the internal representations of pretrained transformers resemble their saturated counterparts, whereas for randomly initialized transformers, they do not. This suggests that the norm growth implicit in training guides transformers toward finding solutions resembling saturated networks, justifying saturated network analysis (Merrill, 2019) as a method for exploring the inductive biases of NLP architectures.

Component	$k$ Input	$k$ Output
Linear	$k$	$k + 1$
Bias	1	1
Affine	0	1
LayerNorm	$k$	0
LayerNorm + Affine	$k$	1
ReLU	$k$	$k$
Sum	$(k, k)$	$k$
Product	$(k_1, k_2)$	$k_1 + k_2$

Table 1: Effects of network components on homogeneity shown by Li and Arora (2019). We write the output homogeneity “ $k$  Output” as a function of the input homogeneity “ $k$  Input”. These facts can be applied to a network graph to compute the homogeneity (if it exists) of a larger network. In Appendix A, we show the same relations hold for *approximate* homogeneity.

**Roadmap** In Section 2, we introduce relevant formal definitions. In Section 3, we link infinite norm growth to saturation and explore the dynamics of the norm during training. In Section 4, we develop the connection between norm growth and training accuracy through both theoretical analysis and experiments. Finally, in Section 5, we investigate norm growth and saturation in pretrained transformers. All proofs are in the appendices.

## 2 Preliminaries

Let  $f(x; \theta)$  be a neural network with inputs  $x$  and weights  $\theta$ . We formally define saturation, which was introduced informally in Section 1.

**Definition 1** (Saturation; Merrill et al., 2020) Given a network  $f(x; \theta)$ , the *saturated network*  $s\text{-}f(x; \theta)$  is defined

$$s\text{-}f(x; \theta) = \lim_{c \rightarrow \infty} f(x; c\theta).$$

An important notion introduced by Li and Arora (2019, Appendix C) is *scale invariance*, which means a parameterized function’s value does not change when its parameters are uniformly scaled.

**Definition 2** (Scale invariance; Li and Arora, 2019) A function  $f(x; \theta)$  is *scale-invariant* in  $\theta$  if for all  $c \geq 1$ , inputs  $x$ , and parameters  $\theta$ ,  $f(x; c\theta) = f(x; \theta)$ .

Li and Arora (2019) observe that, for any scale-invariant loss  $L$ ,  $\theta^\top \cdot \frac{\partial L}{\partial \theta} = 0$ . They show that, because of this property, the norm will grow during training for a scale-invariant network. We will call the quantity  $\theta^\top \cdot \frac{\partial L}{\partial \theta}$  the *gradient projection*.

Scale invariance naturally relates to saturation: for a scale-invariant network, the saturated capacity is equivalent to the full capacity, as scaling the weights to  $\infty$  does not change the network behavior.

**Definition 3** (Homogeneity) A function  $f(x; \theta)$  is  *$k$ -homogeneous* in  $\theta$  if for all  $c \geq 1$ ,  $f(x; c\theta) = c^k f(x; \theta)$ . Note that scale invariance is equivalent to 0-homogeneity.

We say that a function is homogeneous to mean “ $k$ -homogeneous for some  $k$ ”. As argued by Li and Arora (2019), many components of modern neural networks are homogeneous. They show how various functions in the network transform the homogeneity, expressing the homogeneity of their output as a function of their input (in certain cases, the homogeneity of the output is undefined). These effects are summarized in Table 2. Applying these facts over the full network graph, we can recursively compute  $k$  for the full network (which is potentially undefined if some component of the network is not homogeneous).

While scale invariance and homogeneity are useful tools for characterizing some network components, they fall short of characterizing all the common pieces of neural networks. For example, the output homogeneity of softmax is, strictly speaking, undefined. To extend these tools to softmax and other network components, we relax the definition to *approximate* scale invariance and homogeneity. Here and throughout the paper, we will make use of asymptotic  $\mathcal{O}$ ,  $\Omega$ , and  $\Theta$  notation.

**Definition 4** (Approximate homogeneity) A function  $f(x; \theta)$  is *approximately  $k$ -homogeneous* in  $\theta$  if its scaling error vanishes exponentially in  $\|\theta\|$ , i.e., for all  $c \geq 1$  and  $\theta$ ,

$$|f(x; c\theta) - c^k f(x; \theta)| \leq \exp(-\Omega(\|\theta\|)). \quad (1)$$

We define approximate scale invariance as approximate 0-homogeneity. In Appendix A, we show that the properties in Table 2 transform approximate homogeneity the same as strict homogeneity.

Using these results, we then show in Appendix B that transformer sublayers preserve approximate homogeneity.<sup>1</sup>

### 3 Norm Dynamics

Motivating our study of norm growth is the following result, which we interpret as saying that parameter norm growth across the network guides GD towards saturated networks. Thus, saturation is not just a method for simplifying deep learning architectures, but a state that certain training procedures will approach in the infinite-time limit.

**Theorem 1** (Restated in Corollary 9.1) *Let  $\theta(t) \in \mathbb{R}^n$  be the parameter vector of a network  $f(x; \theta(t))$  for  $t$  over the course of training. By  $\theta_i(t)$  we denote a specific scalar parameter. For each  $i, j$ , as  $t \rightarrow \infty$ , assume that  $|\theta_i(t)| \rightarrow \infty$  and  $\theta_i(t)/\theta_j(t)$  converges. Then  $f$  converges to a saturated network as  $t \rightarrow \infty$ .*

There are two assumptions here. One is that each parameter continues to grow (and does not converge) in magnitude. The other is that the ratio between each parameter eventually converges. This is similar to saying that the direction of the parameter vector converges, with the added constraint that no parameter asymptotically dominates any other.

Our later empirical study of the parameters of T5 over training relates to these assumptions. Figure 2 suggests that the aggregate parameter norm grows empirically, and it does not appear to converge. Also, it suggests that the condition where each  $\theta_i(t)/\theta_j(t)$  converges is not overly onerous, as by layer the parameters are growing approximately at the same rate, up to a scalar factor. Thus, the conditions for Theorem 1 appear to be satisfied empirically.

We now investigate *why* the dynamics of training should cause the norm to grow. In particular, we show how the quantity  $\theta^\top \cdot \frac{\partial L}{\partial \theta}$  is related to norm growth. We assume that the training process produces a sequence of updates  $\{\delta_t\}_{t=1}^T$  with each  $\delta_t \in \mathbb{R}^n$ . The parameters are updated according to the recurrence  $\theta_{t+1} = \theta_t + \delta_t$ . We study how the norm changes from time  $t$  to  $t + 1$ . Following the derivation in Appendix C of Li and Arora (2019), we expand the square as follows:

$$\|\theta_{t+1}\|^2 = \|\theta_t + \delta_t\|^2 \tag{2}$$

$$= \|\theta_t\|^2 + \|\delta_t\|^2 + 2\theta_t^\top \cdot \delta_t. \tag{3}$$

Assume  $\theta_0 = 0$ . Expanding the recurrence up to time  $t + 1$ , we get

$$\|\theta_{t+1}\|^2 = \sum_{i=1}^t \left( \|\delta_i\|^2 + 2\theta_i^\top \cdot \delta_i \right) \tag{4}$$

$$= \sum_{i=1}^t \|\delta_i\|^2 + 2 \sum_{i=1}^t \theta_i^\top \cdot \delta_i. \tag{5}$$

If  $\theta_t^\top \cdot \delta_t \geq 0$  at some step  $t$ , then the norm is guaranteed not to decrease at  $t + 1$  by (5). Thus, norm monotonically increases when  $\theta_t^\top \cdot \delta_t$  is non-negative. The norm increases maximally when every step  $\delta_t$  is parallel to  $\theta_t$ , i.e., for all  $t$ ,  $\theta_t^\top \cdot \delta_t = \|\theta_t\| \|\delta_t\|$ . Since  $T$  is finite, the step size is bounded by some  $\delta^*$ . In this case,  $\|\theta_t\| \leq t\delta^* = \mathcal{O}(t)$ , which constitutes an upper bound for norm growth.

If  $\theta_t^\top \cdot \delta_t = 0$  for all  $t$ , it follows from (5) that the norm is  $\leq \sqrt{t\delta^*} = \mathcal{O}(\sqrt{t})$ . Thus, the upper bound dynamics in this case resemble the expected trajectory of a random walk. Li and Arora (2019) show that any scale-invariant network satisfies  $\theta_t^\top \cdot \delta_t = 0$  for all  $t$ , and thus exhibit monotonic norm growth bounded by  $\mathcal{O}(\sqrt{t})$ .

Finally, if  $\theta_t^\top \cdot \delta_t$  is negative at step  $t$ , we cannot say for certain that the norm will decrease at time  $t + 1$ , as it depends on the relevant scale of the terms in (3). However, we can establish a lower bound using the case where, for all  $t$ ,  $\delta_t$  points in the opposite direction from  $\theta_t$ , i.e.,  $\theta_t^\top \cdot \delta_t = -\|\theta_t\| \|\delta_t\|$ . Under these conditions, the norm will decrease at most linearly, i.e.,  $-\mathcal{O}(t)$ .

<sup>1</sup>We prove this only when biases and residual connections are removed. However, we find it holds empirically even without simplifying assumptions. This recalls findings of Lyu and Li (2019) with feedforward networks.

For GD-like methods,  $\theta_t^\top \cdot \delta_t$  is proportional to  $-\theta^\top \cdot \frac{\partial L}{\partial \theta}$ . Thus, we will use  $\theta^\top \cdot \frac{\partial L}{\partial \theta}$  as a *diagnostic metric for norm growth*. If it is consistently  $\leq 0$  over some time interval, the norm is increasing, and if it is  $> 0$ , the norm is shrinking. Since the gradient magnitude should shrink over time with GD, we expect that actual norm trajectories of GD to be less steep than the upper bounds discussed here.

## 4 Accuracy and Norm Growth

The  $\theta^\top \cdot \frac{\partial L}{\partial \theta}$  metric reveals an interesting connection between training accuracy and norm growth for homogeneous networks. We show that this metric is negative on a correct prediction (Theorem 2) and positive on an incorrect one (Theorem 3). It follows that training accuracy controls the point at which the parameter norm growth reaches equilibrium, i.e.,  $\theta^\top \cdot \frac{\partial L}{\partial \theta} > 0$ . Thus, achieving higher accuracy allows for more norm growth. We first prove this for homogeneous networks with binary cross-entropy loss, and then show empirically that the relationship between accuracy and norm growth for transformer sublayers is similar. We leave the question of how this trend manifests in full transformers—and the effect of variables like depth and width—to future work.

### 4.1 Homogeneous Networks with Binary Cross-Entropy Loss

We start by analyzing the case where the network is a homogeneous function  $f$  followed by binary cross-entropy loss. This is similar to the case of transformers, with two important simplifications. As discussed in transformers are not strictly homogeneous, but, rather, are approximately homogeneous in the sense described in (4). Second, many practical networks use the multiclass softmax cross-entropy loss instead of binary cross-entropy.

As discussed in Section 3,  $\theta^\top \cdot \frac{\partial L}{\partial \theta}$  is useful for analyzing norm growth, assuming small learning rate. If it is negative, the weights will grow, as the gradient pushes them outwards. If it is positive, there exists some value at which the norm stops increasing, and above which, it shrinks. Thus, the smallest norm where  $\theta^\top \cdot \frac{\partial L}{\partial \theta} > 0$  acts roughly as an equilibrium point where further norm growth is bounded.

We first summarize our results informally. If the network is “right” in its classification, then the gradient projection is negative (and approaching zero for large  $\|\theta\|$ ). On the other hand, if the network is “wrong”, the gradient projection is positive and increasing with  $\|\theta\|$ . Thus, the sign of the batch-level projection depends on accuracy. If training accuracy is 100%, then the projection will be negative throughout training, and the norm will continue to grow. If accuracy is below 100%, then at some point the gradient projection will cross zero, causing norm growth to reach equilibrium. This means that each accuracy level has a specific norm up to which the parameters will grow.

Let  $f(x; \theta)$  be a  $k$ -homogeneous network, and  $L$  the binary cross-entropy loss. Write  $f$  as shorthand for  $f(x; \theta)$ . Define the prediction  $\hat{y} = 1$  if  $f > 0$  and 0 otherwise. Assume  $f \neq 0$ .

**Theorem 2** For a training example  $(x, y)$ , if  $\hat{y} = y$ , then  $\theta^\top \cdot \frac{\partial L}{\partial \theta} \leq \frac{-k|f|}{\exp(\Theta(|f|))} < 0$ .

**Theorem 3** For a training example  $(x, y)$ , if  $\hat{y} \neq y$ , then  $\theta^\top \cdot \frac{\partial L}{\partial \theta} \geq \frac{k|f|}{2} > 0$ .

See Appendix D for proofs of these theorems.

In any batch, the loss used to train the network is a sum of several training instances. Thus, the gradient projection  $\theta^\top \cdot \frac{\partial L}{\partial \theta}$  is also the sum of the “right” negative term and a “wrong” positive term, weighted by accuracy. If accuracy is 100%, then it will reduce to the negative quantity in Theorem 2, guaranteeing continued norm growth. However, if any instances are misclassified, then the two terms both receive nonzero weight. Since the positive term asymptotically dominates the negative one, norm growth will cease after enough time. Thus, each specific accuracy level has a value up to which norm will grow, and increasing the training accuracy increases this threshold.

### 4.2 Transformer Sublayers

For networks with homogeneous logits and binary cross-entropy loss, we have shown that achieving higher levels of training accuracy increases the level to which the norm can grow. We now test experimentally whether the predicted relationship holds for transformer sublayers, which we argue in Appendix B are almost homogeneous, with softmax cross-entropy loss. To do this, we run

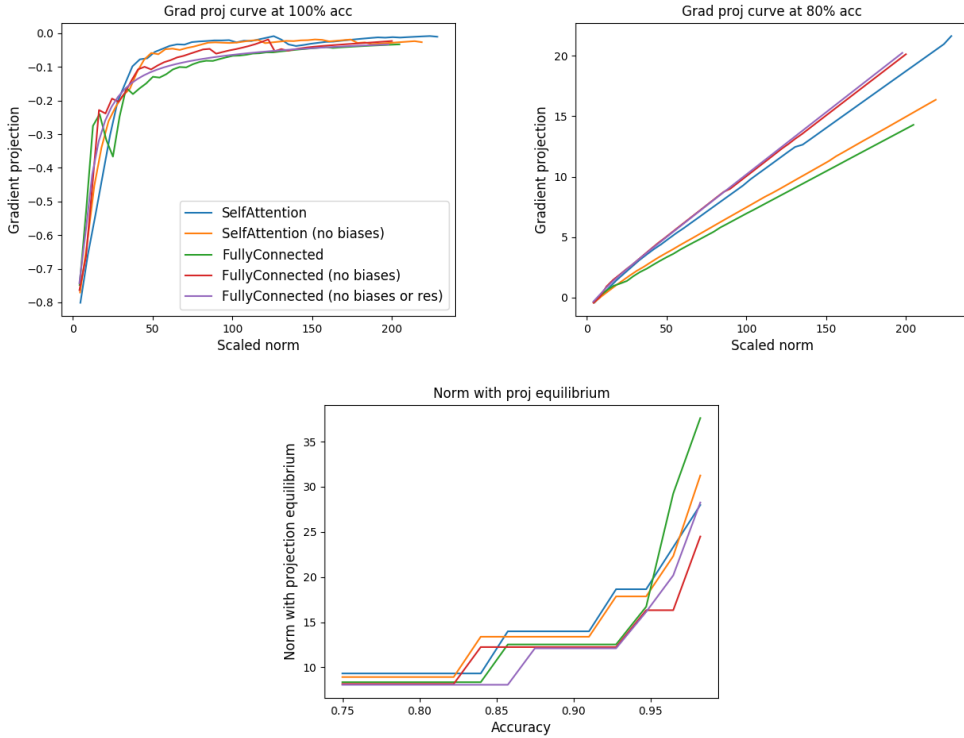


Figure 1: Gradient projection with accuracy fixed at 100% (**left**) and 80% (**right**). The **bottom** shows norm achieving projection equilibrium as a function of accuracy. All plots share a legend.

experiments with randomly initialized transformer components, controlling accuracy by randomly constructing labels. For simplicity, we fix the hidden size of each component to 10.

**Gradient projection curves** First, we visualize the gradient projection curve as a function of norm, at different fixed accuracy levels. We do this for each component of the transformer in isolation. The transformer sublayers (discussed further in Appendix B) are:

- **Self attention sublayer** — we test variants with and without biases.
- **Fully connected sublayer** — we consider three variants: standard, one with biases removed, and one without biases and residual connections.

The reason we consider these variants is that, as discussed in Appendix B, we assume biases and residual connections are removed in our formal analysis of the approximate homogeneity of transformers. However, both here and in Appendix B, we find that transformer components behave similarly with and without these simplifying assumptions.

Given a transformer sublayer, we define the loss by first applying a random affine layer, followed by the softmax cross-entropy loss function. We randomly initialize the parameters, and vary the “scale”  $c \geq 1$  as the independent variable. We pick a fixed accuracy level  $a \in [0, 1]$ . Importantly, we never train the network, computing gradients only for  $\theta^\top \cdot \frac{\partial L}{\partial \theta}$ . For each  $c$ , we do the following:

1. Scale the network parameters by  $c$ , i.e.,  $\theta \mapsto c\theta$ .
2. For each  $x$ , compute  $h = f(x; c\theta)$ .
3. We set fake labels  $y$ . For  $a$  percent of samples, set  $y = \arg \max h$ . For  $(1 - a)$  percent, set  $y$  to a value besides  $\arg \max h$ .
4. Compute and record the dependent variable  $\theta^\top \cdot \frac{\partial L}{\partial \theta}$  using auto-differentiation.

Let  $\rho_0$  be the norm of the randomly initialized parameters. Figure 1 shows  $\theta^\top \cdot \frac{\partial L}{\partial \theta}$  as a function of  $c\rho_0$  at two fixed accuracy levels: 100% and 80%. With fixed 100% accuracy, the projection is always negative and approaches 0. With 80% accuracy, however, the projection becomes positive at a very small norm value, and it increases roughly linearly. Thus, the empirical results for transformer sublayers match the theory for homogeneous networks with binary cross-entropy loss.

**Norm equilibrium by accuracy** We now extend this experiment to plot the norm equilibrium point for a component  $f$  as a function of accuracy. To do this, we construct a random dataset of inputs  $x$ . We then pick various “scales” for the parameters  $c$  and accuracy levels  $a$ . For the pair of independent variables  $(c, a)$ , we use the same method as the previous experiment to compute a sequence of  $\theta^\top \cdot \frac{\partial L}{\partial \theta}$  for each  $a$ . For each  $a$ , we then compute the first scale  $c^*(a)$  in the time series at which  $\frac{\partial L}{\partial \theta} \cdot \theta > 0$ . This corresponds to a specific norm  $\rho^*(a) = c^*(a)\rho_0$  where  $\rho_0$  is the norm of the unscaled parameters. We plot  $\rho^*(a)$  as a function of  $a$  in the bottom plot of Figure 1.

Figure 1 shows that the equilibrium point for  $\theta^\top \cdot \frac{\partial L}{\partial \theta}$  increases with accuracy, as was predicted in the theoretical analysis of homogeneous networks. The norm equilibrium point remains finite for any accuracy  $< 100\%$ , going to infinity for a model that perfectly predicts the training data.

While the theoretical relationship between accuracy and norm holds empirically for transformer sublayers, for full transformers, the effect of variables like depth and width is unclear. Preliminary experiments suggest, for larger networks, the projection may remain  $\sim 0$  even for low accuracies. While Section 5 confirms that the norm continuously grows during pretraining of T5, we leave further analysis of full transformers to future work.

### 4.3 Vanishing Step Size

Theorem 2 implies that, if 100% accuracy is achieved, gradient flow diverges to a saturated network. But, even under these conditions, do GD and related optimizers really approach infinite norm? In this section, we show that the step size towards the saturated network vanishes, causing the norm to converge. While this is not particularly surprising, it suggests we should expect GD to reach “semi-saturated” networks, rather than getting arbitrarily close to a saturated network. This resembles the empirical findings of semi-saturation in LSTMs reported by Shibata et al. (2020).

**Theorem 4** *Let  $f : \mathbb{R}^n \rightarrow \mathbb{R}$  be a  $k$ -homogeneous network followed by binary cross-entropy loss. We assume  $\|\nabla f\|$  is bounded over the  $n$ -sphere. Let  $\rho_t = \|\theta_t\|$ . On training example  $(x, y)$ , if  $\hat{y} = y$ ,*

$$\|\nabla L|_{\theta_t}\| \leq \frac{\mathcal{O}(\rho_t^{k-1})}{\exp(\Omega(\rho_t))}. \quad (6)$$

We restate this in Theorem 12. Theorem 4 suggests the gradient points along a divergent trajectory, but the step size vanishes, leading the distance travelled along the path to converge. However, there still exists a saturated network with 0 loss at the end of the path. While the network found by training is only partially saturated, the existence of this lower-loss saturated network suggests that the saturated capacity might still indirectly bound the solutions found by GD.

## 5 Pretrained Transformers

In this section, we examine the properties of pretrained transformers from the perspective of norm growth. We expect the parameter norm to increase over training, while their normalized direction converges. This should cause the transformer to increasingly approximate its saturated form.

**Norm growth with T5** We evaluate the rate of norm growth using historical checkpoints from the T5-base (Raffel et al., 2019) pretraining process. As reported in the original paper, this model has about 220 trainable parameters. The  $L_2$  parameter norm over time is plotted in the left side of Figure 2. The growth trend resembles  $\sqrt{t}$ , suggesting that  $\theta^\top \cdot \frac{\partial L}{\partial \theta}$  for T5 may be close to 0. We encourage future work pretraining such models to track metrics like parameter norm and  $\theta^\top \cdot \frac{\partial L}{\partial \theta}$ .

The right side of Figure 2 breaks down the trend in norm growth for T5 by layer. Generally, the norm grows at a higher rate for later layers in the transformer than for earlier ones. This suggests different regions of the network do not “saturate” at the same rate.

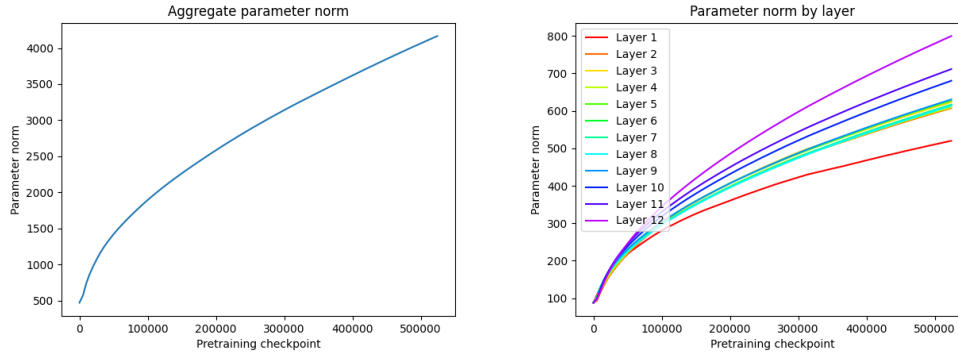


Figure 2: Growth in parameter norm during T5 pretraining (**left**), broken down by layer on the **right**.

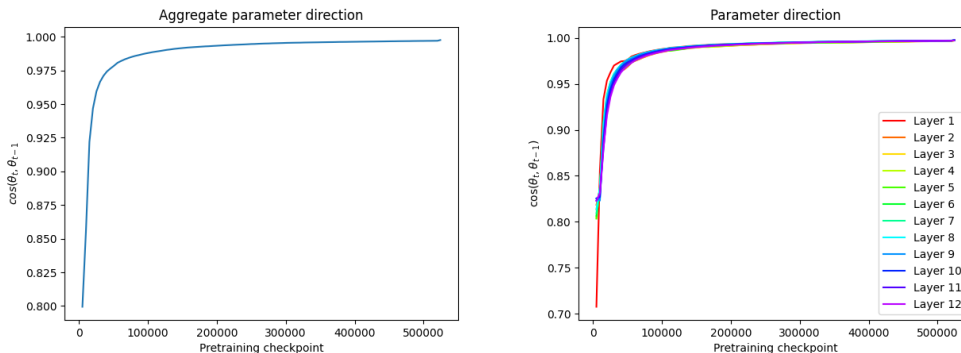


Figure 3: Cosine similarity between parameters of subsequent checkpoints during T5 pretraining (**left**). The same trend broken down by layer (**right**).

**Directional convergence** In Figure 3, we look at the cosine similarity between the T5 parameters at one checkpoint and the previous checkpoint. A similarity close to 1 means the parameters point in the same direction at subsequent steps. This suggests that  $\theta_i(t)/\theta_j(t)$  does not oscillate, and therefore is likely to converge over the course of training (cf. Theorem 1).

**How saturated are pretrained transformers?** We argue in Appendix B that transformer components are approximately 1-homogeneous for large enough norm. Thus, the representations of a transformer with large norm are a scalar multiple of the representations from a saturated network. We therefore expect high cosine similarity between saturated and unsaturated transformer representations.

We estimate this *representation similarity* as  $\frac{f_\theta(x) \cdot f_{c\theta}(x)}{\|f_\theta(x)\| \|f_{c\theta}(x)\|}$  for some large  $c$  (in our case 1000). We compute the mean of this measure over 100 input sentences from the Brown corpus (Francis and Kučera, 1989). To conform with standard practice, each sentence is truncated at 512 word pieces. We compare the value of this metric at each layer of the “base” versions of BERT, RoBERTa, T5, and XLNet. We compare the values for the pretrained models against a randomly reinitialized baseline.

Figure 4 compares the representation similarity throughout the network for randomly initialized transformers and pretrained transformers. For every model type, the similarity is higher for the pretrained network than the randomly initialized network, which, except for T5, is close to 0. For RoBERTa, the cosine similarity of the final representation is  $\sim 0.6$ , and for T5 and XLNet,  $\sim 0.9$ . For T5 and XLNet, similarity is higher in later layers, which is potentially surprising, as one might expect error to compound with more layers. This may be related to the fact that the norm grows faster for later layers in T5. One puzzle is why the similarity for BERT is much lower than these models. As RoBERTa is architecturally similar to BERT, with the major difference being RoBERTa was pretrained for more steps, we hypothesize RoBERTa’s higher similarity is due to longer pretraining.



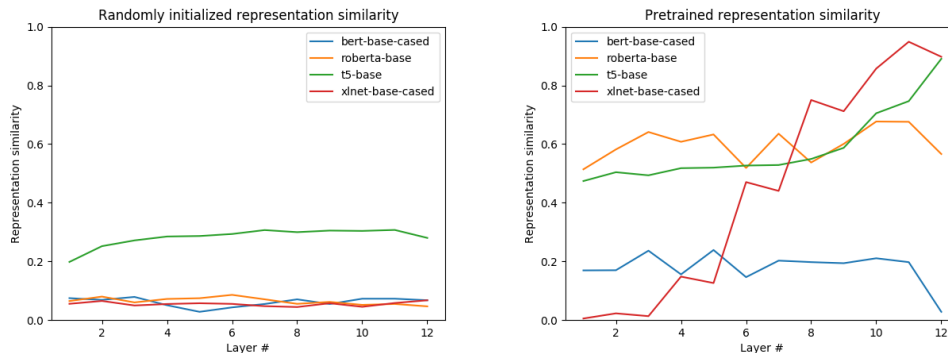


Figure 4: Cosine similarities of the unsaturated and saturated ( $c = 1000$ ) transformer representations, by layer. We compare randomly initialized transformers (**left**) to pretrained ones (**right**).

## 6 Conclusion

**Cause of norm growth** Theorem 1 reveals that training approaches a saturated network if the parameters diverge in norm but converge in direction. Empirically, we find that the norm does continuously grow during T5 pretraining, and the direction converges. In Section 4, we ask why the parameter norm should grow while training transformers. We leverage the fact that transformers are approximately homogeneous to show that norm growth increases with performance on the training set, both in a simplified formal model, and empirically for transformer sublayers. We present the intuition that there exists a ball in parameter space of *gradient projection equilibrium*, which expands as accuracy increases. It is unclear how this relationship is affected by variables like depth and width in larger networks—a question we leave to future work.

**Effect of norm growth** We show that common pretrained language models become approximately saturated through pretraining, and models that have been trained for longer appear to saturate more. While we lack a precise formal characterization of the capacities of “semi-saturated” transformers, we conjecture that the capacities of such models resemble those of the saturated models. Further, for models with 100% accuracy, full saturation is not achieved because the step size eventually vanishes. In some sense, vanishing step size is an artifact of designing optimizers to find local minima, rather than good trajectories. Existing optimizers could be modified to remove this effect, for example, by normalizing the step. We leave open the question of how making these changes—and thus reaching more saturated networks—affects the performance of practical neural networks.

While we focus on transformers, Theorem 1 generally shows that unbounded norm growth leads to saturation for *any* network. Our results in Section 4 assume homogeneity—a property met approximately by a variety of neural architectures, not just transformers. Thus, we hope these theoretical results advance the general understanding of neural network training dynamics.

## Acknowledgments and Disclosure of Funding

Thanks to Colin Raffel for providing access to the T5 training checkpoints. Further, thanks to researchers at the Allen Institute for AI for feedback and suggestions.

## References

- S. Arora, N. Cohen, W. Hu, and Y. Luo. Implicit regularization in deep matrix factorization, 2019.
- S. Bhattamishra, K. Ahuja, and N. Goyal. On the ability of self-attention networks to recognize counter languages, 2020.
- J. Devlin, M.-W. Chang, K. Lee, and K. Toutanova. BERT: Pre-training of deep bidirectional transformers for language understanding. In *Proceedings of the 2019 Conference of the North American Chapter of the Association for Computational Linguistics: Human Language Technologies, Volume 1 (Long and Short*

- Papers*), pages 4171–4186, Minneapolis, Minnesota, June 2019. Association for Computational Linguistics. doi: 10.18653/v1/N19-1423. URL <https://www.aclweb.org/anthology/N19-1423>.
- W. N. Francis and H. Kučera. *Manual of information to accompany a standard corpus of present-day edited American English, for use with digital computers*. Brown University, Department of Linguistics, 1989.
- S. Gunasekar, B. Woodworth, S. Bhojanapalli, B. Neyshabur, and N. Srebro. Implicit regularization in matrix factorization, 2017.
- M. Hahn. Theoretical limitations of self-attention in neural sequence models. *Transactions of the Association for Computational Linguistics*, 8:156–171, Jan 2020. ISSN 2307-387X. doi: 10.1162/tacl\_a\_00306. URL [http://dx.doi.org/10.1162/tacl\\_a\\_00306](http://dx.doi.org/10.1162/tacl_a_00306).
- C. Kirov and R. Frank. Processing of nested and cross-serial dependencies: an automaton perspective on SRN behaviour. *Connection Science*, 24(1):1–24, 2012. doi: 10.1080/09540091.2011.641939. URL <https://doi.org/10.1080/09540091.2011.641939>.
- Z. Li and S. Arora. An exponential learning rate schedule for deep learning. In *Proc. of ICLR*, 2019.
- Y. Liu, M. Ott, N. Goyal, J. Du, M. Joshi, D. Chen, O. Levy, M. Lewis, L. Zettlemoyer, and V. Stoyanov. Roberta: A robustly optimized bert pretraining approach, 2019.
- K. Lyu and J. Li. Gradient descent maximizes the margin of homogeneous neural networks, 2019.
- W. Merrill. Sequential neural networks as automata. *Proceedings of the Workshop on Deep Learning and Formal Languages: Building Bridges*, 2019. doi: 10.18653/v1/w19-3901. URL <http://dx.doi.org/10.18653/v1/w19-3901>.
- W. Merrill, G. G. Weiss, Y. Goldberg, R. Schwartz, N. A. Smith, and E. Yahav. A formal hierarchy of RNN architectures. *ArXiv*, abs/2004.08500, 2020.
- M. S. Nacson, S. Gunasekar, J. D. Lee, N. Srebro, and D. Soudry. Lexicographic and depth-sensitive margins in homogeneous and non-homogeneous deep models, 2019.
- T. Poggio, A. Banburski, and Q. Liao. Theoretical issues in deep networks: Approximation, optimization and generalization, 2019.
- T. Poggio, Q. Liao, and A. Banburski. Complexity control by gradient descent in deep networks. *Nature communications*, 11(1):1–5, 2020.
- C. Raffel, N. Shazeer, A. Roberts, K. Lee, S. Narang, M. Matena, Y. Zhou, W. Li, and P. J. Liu. Exploring the limits of transfer learning with a unified text-to-text transformer, 2019.
- N. Razin and N. Cohen. Implicit regularization in deep learning may not be explainable by norms, 2020.
- C. Shibata, K. Uchiumi, and D. Mochihashi. How lstm encodes syntax: Exploring context vectors and semi-quantization on natural text, 2020.
- H. T. Siegelmann and E. D. Sontag. On the computational power of neural nets. In *Proc. of COLT*, pages 440–449, 1992. ISBN 0-89791-497-X. doi: 10.1145/130385.130432. URL <http://doi.acm.org/10.1145/130385.130432>.
- M. Suzgun, Y. Belinkov, S. Shieber, and S. Gehrmann. LSTM networks can perform dynamic counting. In *Proceedings of the Workshop on Deep Learning and Formal Languages: Building Bridges*, pages 44–54, Aug. 2019a. URL <https://www.aclweb.org/anthology/W19-3905>.
- M. Suzgun, S. Gehrmann, Y. Belinkov, and S. M. Shieber. Memory-augmented recurrent neural networks can learn generalized Dyck languages, 2019b.
- A. Vaswani, N. Shazeer, N. Parmar, J. Uszkoreit, L. Jones, A. N. Gomez, L. Kaiser, and I. Polosukhin. Attention is all you need, 2017.
- G. Weiss, Y. Goldberg, and E. Yahav. On the practical computational power of finite precision RNNs for language recognition, 2018. URL <http://arxiv.org/abs/1805.04908>.
- T. Wolf, L. Debut, V. Sanh, J. Chaumond, C. Delangue, A. Moi, P. Cistac, T. Rault, R. Louf, M. Funtowicz, and J. Brew. Huggingface’s transformers: State-of-the-art natural language processing. *ArXiv*, abs/1910.03771, 2019.
- Z. Yang, Z. Dai, Y. Yang, J. Carbonell, R. Salakhutdinov, and Q. V. Le. Xlnet: Generalized autoregressive pretraining for language understanding, 2019.

## A Approximate Homogeneity

Note that if  $f(\theta)$  is approximately  $k$ -homogeneous, then  $f(c\theta) = c^k f(\theta) + \epsilon$  for some error vector  $\epsilon$  where, for each  $i$ ,  $|\epsilon_i| \leq \exp(-\Omega(\|\theta\|))$ . We use this  $\epsilon$  notation throughout this section.

### A.1 Consistency

We first prove that approximate homogeneity is consistent: in other words, if a function is both approximately  $k_1$  and  $k_2$ -homogeneous, then  $k_1 = k_2$ . This is an important property for establishing approximate homogeneity as a meaningful notion.

**Lemma 1** *Let  $k_1, k_2 \in \mathbb{N}$ . Assume that  $f$  is both approximately  $k_1$  and  $k_2$ -homogeneous. Then  $k_1 = k_2$ .*

*Proof.* If  $f$  is both approximately  $k_1$  and  $k_2$ -homogeneous, then we have vanishing terms  $\epsilon_1$  and  $\epsilon_2$  such that, for all  $c$ ,

$$f(c\theta) = c^{k_1} f(\theta) + \epsilon_1 \quad (7)$$

$$f(c\theta) = c^{k_2} f(\theta) + \epsilon_2. \quad (8)$$

Subtracting both sides yields

$$0 = (c^{k_1} - c^{k_2})f(\theta) + \epsilon_1 - \epsilon_2 \quad (9)$$

$$\therefore |c^{k_1} - c^{k_2}| = \frac{|\epsilon_1 - \epsilon_2|}{|f(\theta)|}. \quad (10)$$

The right-hand side vanishes exponentially in  $\|\theta\|$ , whereas the left-hand side grows with  $c$  unless  $k_1 = k_2$ . Thus, to satisfy (10) for all  $c$ , it must be the case that  $k_1 = k_2$ .  $\square$

### A.2 Closure Properties

We now prove that effects of various functions on homogeneity explored by Li and Arora (2019) also translate to approximate homogeneity.

**Lemma 2** *ReLU preserves approximate  $k$ -homogeneity, i.e., let  $f : \mathbb{R}^n \rightarrow \mathbb{R}$  be approximately  $k$ -homogeneous. Then  $\text{ReLU} \circ f$  is approximately  $k$ -homogeneous.*

*Proof.*

$$\text{ReLU}(f(c\theta)) = \text{ReLU}(c^k f(\theta) + \epsilon) \quad (11)$$

$$\leq \text{ReLU}(c^k f(\theta)) + |\epsilon|. \quad (12)$$

Therefore,

$$\left| \text{ReLU}(f(c\theta)) - \text{ReLU}(c^k f(\theta)) \right| \leq |\epsilon|. \quad (13)$$

Set  $\epsilon' = |\epsilon|$ , showing  $\text{ReLU}(f(\theta))$  is approximately  $k$ -homogeneous.  $\square$

**Lemma 3** *Let  $f, g$  be vector-valued functions of  $\theta$ . If  $f$  and  $g$  are approximately  $k$ -homogeneous, then  $f + g$  is approximately  $k$ -homogeneous.*

*Proof.*

$$f(c\theta) + g(c\theta) = c^k f(\theta) + \epsilon_f + c^k g(\theta) + \epsilon_g \quad (14)$$

$$= c^k f(\theta) + c^k g(\theta) + \epsilon', \quad (15)$$

where  $\epsilon' = \epsilon_f + \epsilon_g$ . Thus,

$$\left| f(c\theta) + g(c\theta) - c^k (f(\theta) + g(\theta)) \right| \leq \epsilon'. \quad (16)$$

$\square$

**Lemma 4** *Let  $f, g$  be vector-valued functions of  $\theta$ . If  $f$  and  $g$  are approximately  $k_f$  and  $k_g$ -homogeneous, then  $f \cdot g$  is approximately  $(k_f + k_g)$ -homogeneous.*

*Proof.*

$$f(c\theta) \cdot g(c\theta) = (c_f^k f(\theta) + \epsilon_f) \cdot (c_g^k g(\theta) + \epsilon_g) \quad (17)$$

$$= c^{k_f+k_g} f(\theta)g(\theta) + c_f^k f(\theta)\epsilon_g + c_g^k g(\theta)\epsilon_f + \epsilon_f\epsilon_g \quad (18)$$

Since  $f(\theta) = \exp(\log f(\theta))$ , the second and third terms are bounded by a vanishing exponential. The fourth term is also similarly bounded. Thus, there exists  $\epsilon'$  bounding the sum of these three terms. We obtain

$$\left| f(c\theta)g(c\theta) - c^{k_f+k_g} f(\theta)g(\theta) \right| \leq \epsilon'. \quad (19)$$

□

The analogous results for linear transformation, bias, and affine transformation directly follow from the results for sum and product in Lemma 3 and Lemma 4.

Finally, we show that layer norm converts a homogeneous function to approximately scale-invariant function. In order to be numerically stable, practical implementations of layer norm utilize a small error term so that the denominator is never zero. We omit this practical detail from our analysis, instead defining the layer norm  $\text{LN}(x)$  for  $x \in \mathbb{R}^n$  according to

$$\mu(x) = \frac{1}{n} \sum_{i=1}^n x_i \quad (20)$$

$$\text{LN}(x)_i = \frac{x_i - \mu(x)}{\|x - \mu(x)\|}. \quad (21)$$

**Lemma 5** *Let  $f$  be approximately  $k$ -homogeneous for some  $k$ . Then,  $\text{LN}(f)$  is approximately 0-homogeneous.*

*Proof.* Since addition preserves approximate  $k$ -homogeneity, mean (and difference to mean), preserve approximate  $k$ -homogeneity. Letting  $C = c^k$ , we can write

$$f(c\theta) - \mu(f(c\theta)) = C(f(\theta) - \mu(f(\theta))) + \epsilon. \quad (22)$$

We now apply this to the definition of layer norm to get

$$\text{LN}(f(c\theta))_i = \frac{f(c\theta)_i - \mu(f(c\theta))}{\|f(c\theta) - \mu(f(c\theta))\|} \quad (23)$$

$$= \frac{C(f(\theta)_i - \mu(f(\theta))) + \epsilon_i}{C\|f(\theta) - \mu(f(\theta))\| + \epsilon}. \quad (24)$$

We show that the difference between this and the unscaled layer norm goes to zero. To simplify notation, we now write  $f = f(\theta)$ ,  $\mu = \mu(f(\theta))$ , and  $\epsilon = \epsilon$  in the left-hand side below:

$$|\text{LN}(f(c\theta))_i - \text{LN}(f(\theta))_i| = \left| \frac{C(f_i - \mu) + \epsilon_i}{C\|f - \mu\| + \epsilon} - \frac{f_i - \mu}{\|f - \mu\|} \right| \quad (25)$$

$$= \left| \frac{C(f_i - \mu)\|f - \mu\| + \epsilon_i\|f - \mu\| - C(f_i - \mu)\|f - \mu\| - \epsilon(f_i - \mu)}{C\|f - \mu\|^2 + \epsilon\|f - \mu\|} \right| \quad (26)$$

$$= \left| \frac{\epsilon_i\|f - \mu\| - \epsilon(f_i - \mu)}{C\|f - \mu\|^2 + \epsilon\|f - \mu\|} \right| \quad (27)$$

$$= \left| \frac{\epsilon_i - \epsilon v}{C\|f - \mu\| + \epsilon} \right|, \quad (28)$$

for some  $v \in \mathbb{R}^n$  which does not grow with  $\|\theta\|$ . Thus, setting  $\epsilon'$  to the quantity in (28) satisfies the definition of approximate 0-homogeneity, i.e. approximate scale invariance. □

### A.3 Saturating Activation Functions

We show that the exponentially saturation activation functions  $\sigma$ , softmax, and tanh are approximately scale-invariant in  $x$ , i.e. scaling  $x$  has an exponentially diminishing effect on the output. We start by analyzing the simpler sigmoid, and then show that the same result holds for softmax. For completeness, we then present a proof for tanh. Recall that we use  $\Theta$  (not  $\theta$ ) in the standard sense of asymptotic notation.

**Lemma 6** *The scaling error for  $\sigma$  vanishes exponentially in the preactivation magnitude, i.e. for all  $c \geq 1$ ,*

$$|\sigma(cx) - \sigma(x)| \leq \Theta(\exp(-|x|)). \quad (29)$$

*Proof.* Assume without loss of generality that  $x \neq 0$ , as if this is the case, the error is 0. When  $x > 0$ , we have

$$|\sigma(cx) - \sigma(x)| = \sigma(cx) - \sigma(x) \quad (30)$$

$$\leq 1 - \sigma(|x|) \quad (31)$$

$$= \frac{1}{\exp(|x|) + 1} \quad (32)$$

$$= \Theta(\exp(-|x|)). \quad (33)$$

When  $x < 0$ , we have

$$|\sigma(cx) - \sigma(x)| = \sigma(x) - \sigma(cx) \quad (34)$$

$$\leq 1 - \sigma(|x|) + 0 \quad (35)$$

$$= \Theta(\exp(-|x|)). \quad (36)$$

□

**Lemma 7** *The elementwise scaling error for softmax vanishes exponentially in the preactivation norm, i.e. for all  $c \geq 1$ ,  $x \in \mathbb{R}^n$  s.t.  $1 \leq i \leq n$ ,*

$$|\text{softmax}(cx)_i - \text{softmax}(x)_i| \leq \exp(-\Theta(\|x\|)). \quad (37)$$

*Proof.* The proof closely follows that of Lemma 6, but is more involved. We consider two cases:  $x_i = \max(x)$ , and  $x_i \neq \max(x)$ .

**Case 1**  $x_i = \max(x)$ .

$$|\text{softmax}(cx)_i - \text{softmax}(x)_i| = \text{softmax}(cx)_i - \text{softmax}(x)_i \quad (38)$$

$$\leq 1 - \text{softmax}(x)_i \quad (39)$$

$$= 1 - \frac{\exp(x_i)}{\sum_j \exp(x_j)} \quad (40)$$

$$\leq 1 - \frac{\exp(\max(x))}{\exp(\max(x)) + (n-1)\exp(\min(x))} \quad (41)$$

$$= 1 - \frac{1}{1 + (n-1)\exp(\min(x) - \max(x))} \quad (42)$$

$$= 1 - \frac{1}{1 + \exp(\min(x) - \max(x) + d)} \quad (43)$$

for some  $d \in \mathbb{R}$ . As (43) has the form of  $\sigma$ , we conclude

$$|\text{softmax}(cx)_i - \text{softmax}(x)_i| = 1 - \sigma(\Theta(\|x\|)) = \exp(-\Theta(\|x\|)). \quad (44)$$

**Case 2**  $x_i \neq \max(x)$ .

$$|\text{softmax}(cx)_i - \text{softmax}(x)_i| = \text{softmax}(x)_i - \text{softmax}(cx)_i \quad (45)$$

$$\leq 1 - \max(\text{softmax}(x)) - 0 \quad (46)$$

$$= 1 - \text{softmax}(\max(x)), \quad (47)$$

which is identical to (39). Thus, the same sequence of steps reaches (44). □

Finally, for completeness, we show that tanh exhibits the same property. The proof is very similar to sigmoid, following closely from the definition

$$\tanh(x) = \frac{\exp(2x) - 1}{\exp(2x) + 1}. \quad (48)$$

**Lemma 8** *The scaling error for tanh vanishes exponentially in the preactivation magnitude, i.e. for all  $c \geq 1$ ,*

$$|\tanh(cx) - \tanh(x)| \leq \exp(-\Theta(|x|)). \quad (49)$$

*Proof.*

$$|\tanh(cx) - \tanh(x)| \leq |1 - \tanh(x)| \tag{50}$$

$$= 1 - \tanh(|x|) \tag{51}$$

$$= 1 - \frac{\exp(2|x|) - 1}{\exp(2|x|) + 1} \tag{52}$$

$$= \frac{\exp(2|x|) + 1 - \exp(2|x|) + 1}{\exp(2|x|) + 1} \tag{53}$$

$$= \frac{2}{\exp(2|x|) + 1} \tag{54}$$

$$= \exp(-\Theta(|x|)). \tag{55}$$

□

Thus, applying these functions to a homogeneous input produces an output that is approximately scale-invariant in the parameters  $\theta$ . Thus, these functions act similarly to layer norm, which maps homogeneous input to scale-invariant output. But what happens if the input is *approximately* homogeneous, rather than strictly homogeneous? In this case, we show that the output is approximately scale-invariant assuming  $\|\theta\|$  is sufficiently large.

**Theorem 5** *Let  $f(x; \theta)$  be approximately  $k$ -homogeneous in  $\theta$ . Then the following functions are approximately scale-invariant in  $\theta$ :*

$$g_\sigma = \sigma \circ f \tag{56}$$

$$g_{\text{softmax}} = \text{softmax} \circ f \tag{57}$$

$$g_{\tanh} = \tanh \circ f. \tag{58}$$

*Proof.* If  $f(x; \theta)$  is approximately  $k$ -homogeneous, then  $f(x; c\theta) = c^k f(x; \theta) + \epsilon$  where  $\|\epsilon\| \leq \exp(-O(\|\theta\|))$ . Crucially, since  $\epsilon$  vanishes for large norm, there is some  $\rho$  where, for all  $\theta$  such that  $\rho < \|\theta\|$ :

$$\text{sgn}(c^k f(x; \theta) + \epsilon) = \text{sgn}(c^k f(x; \theta)) \tag{59}$$

$$\arg \max(c^k f(x; \theta) + \epsilon) = \arg \max(c^k f(x; \theta)). \tag{60}$$

Therefore, for  $\theta$  such that  $\|\theta\| > \rho$ , the bounds used in Lemma 6, Lemma 7, and Lemma 8 hold for approximately homogeneous  $f$ . Thus, we can conclude that the output is approximately scale-invariant. □

## B Transformers

In this section, we show that the transformer encoder is approximately 1-homogeneous. A transformer Vaswani et al. (2017) is made up of three main components: an embedding layer, self attention sublayers, and feed-forward sublayers. Since the embedding layer is just a matrix multiplication, it is a 1-homogeneous function of the input. Assuming the self attention and feed-forward sublayers have no bias terms, we show that they approximate functions preserving 1-homogeneity. As the full network is an initial embedding layer followed by these sublayers, the final output is approximately 1-homogeneous. We argue later in the paper that this important implications for norm growth.

We base our analysis on the HuggingFace implementation<sup>2</sup> of BERT (Wolf et al., 2019). To aid analysis, we make some simplifying assumptions, which are discussed along with the definitions. We later show empirically that homogeneity for the unsimplified versions is similar.

Let  $\text{LN}(\cdot)$  denote a layer norm followed by a learned affine transformation.

**Definition 5** (Self-attention head) Given parameters  $W^k, W^q, W^v$  and input  $X \in \mathbb{R}^{Tn}$ , we define a *self-attention head SA* as

$$K = W^k X \tag{61}$$

$$Q = W^q X \tag{62}$$

$$V = W^v X \tag{63}$$

$$A = \text{softmax}(QK^\top / \sqrt{d_k}) \tag{64}$$

$$H = AV, \tag{65}$$

where  $H$  is the output tensor.

<sup>2</sup>[https://huggingface.co/transformers/\\_modules/transformers/modeling\\_bert.html#BertModel](https://huggingface.co/transformers/_modules/transformers/modeling_bert.html#BertModel)

Compared to the self-attention sublayer of BERT, our simplified version lacks bias terms.

**Theorem 6** *If  $X$  is approximately 1-homogeneous in parameters  $\theta$ , then there exists  $\rho$  such that for all  $\theta$  with  $\rho < \|\theta\|$ ,  $\text{SA}(X; W^k, W^q, W^v)$  is approximately 1-homogeneous in the concatenation of  $\theta, W^k, W^q, W^v$ .*

*Proof.* Consider a self-attention layer receiving a 1-homogeneous input matrix  $X \in \mathbb{R}^{T \times n}$  where  $T$  is the sequence length. Using the homogeneity rule for multiplication,  $K, Q, V$  are each approximately 2-homogeneous, as homogeneity is additive over multiplication. By the same argument,  $QK^\top$  is 4-homogeneous. In Theorem 5, we show there exists  $\rho$  such that, if the input is approximately homogeneous in parameters with norm greater than  $\rho$ , then the output is approximately scale-invariant. Thus,  $A$  is approximately 0-homogeneous for large enough norm. We continue assuming the norm is sufficiently large. Then  $AV$  is approximately 1-homogeneous.  $\square$

We show that the small component that aggregates multiple heads into a shared representation also preserves approximate 1-homogeneity.

**Definition 6** (Multi-head self-attention sublayer) Let  $X \in \mathbb{R}^{T \times n}$  be the input. We now define the  $k$ -multi-head self-attention sublayer  $\text{MSA}_k$ . First, we compute  $k$  self-attention heads in parallel to produce  $H_1, \dots, H_k$ . We then concatenate these along the feature axis to form  $H$ , and compute the sublayer output  $Y$  as

$$Y = \text{LN}(WH + b) \tag{66}$$

Our multi-head mechanism is simplified in that it omits the residual connection in the computation of  $Y$  that exist in BERT.

**Theorem 7** *If  $X$  is approximately 1-homogeneous in parameters  $\theta$ , then there exists  $\rho$  such that for all  $\theta$  with  $\rho < \|\theta\|$ ,  $\text{MSA}$  is approximately 1-homogeneous in the full parameters.*

*Proof.* A bias immediately preceding layer norm has no effect on the network computation. Thus,  $\text{LN}(WH + b) = \text{LN}(WH)$ . Since  $Wh$  is 2-homogeneous,  $\text{LN}(WH)$  is 1-homogeneous.  $\square$

We now turn to analyzing the feedforward sublayer of the transformer. We simplify this sublayer by removing biases and residual connections.

**Definition 7** (Feedforward sublayer) Let  $X \in \mathbb{R}^{T \times n}$  be the input. We compute the *feedforward sublayer* FF according to

$$\text{LN}(W^f \text{ReLU}(W^i x)). \tag{67}$$

**Theorem 8** *If  $X$  is approximately 1-homogeneous, then  $\text{FF}(X; W^f, W^i)$  is approximately 1-homogeneous in the full parameters.*

*Proof.* Multiplying by each  $W$  increases approximate homogeneity by 1, and ReLU preserves approximate homogeneity. So the input to LN is approximately 3-homogeneous. Thus, its output is approximately 1-homogeneous.  $\square$

## B.1 Removing Assumptions

We have theoretically investigated approximate homogeneity for a simplified version of the transformer. In Figure 5 we empirically compare the simplified and non-simplified components, plotting the cosine similarity of the network output to the output when the parameters are scaled by a constant  $c$ . Varying  $c$ , we show that every variant of both components follows an exponential-looking saturation curve. Thus, it appears that the actual transformer components, not just our slightly simplified versions of them, are approximately homogeneous.

It is an interesting puzzle why networks with biases behave similarly to those without biases in terms of homogeneity properties. Lyu and Li (2019) raise a similar point focusing on the homogeneity of feedforward networks.

## C Uniform and Non-Uniform Saturation

The standard definition of saturation from Merrill et al. (2020) assumes uniform norm growth, i.e. a single  $c$  scaling *all* of the parameters. Our empirical study of norm growth in T5, however, shows that the norm is growing at different rates in different parts of the network. This begs the question: is the capacity of a network that saturates uniformly equivalent to the capacity of a network where the parameters go to infinity at different rates? In this section, we investigate this question, and answer in the affirmative. Approaching infinite norm with different rates at each neuron produces the same family of infinite norm networks as uniform saturation.

We first revisit the definition of standard, “uniform” saturation from Merrill et al. (2020):

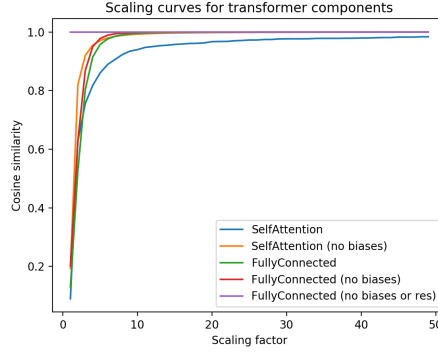


Figure 5: An empirical measure of the homogeneity of various components. The  $x$  axis represents the coefficient by which the parameters in the module is scaled, and the  $y$  axis represents the similarity to the same module scaled by 1000.

**Definition 8** (Uniform saturation) For a network  $f(x; \theta)$ , the *uniform saturated capacity*  $\mathcal{F}_u$  is the set of functions of  $x$  of the following form, over all possible  $\theta$ :

$$f_u(x; \theta) = \lim_{c \rightarrow \infty} f(x; c\theta). \quad (68)$$

On the other hand, the non-uniform saturated capacity allows each neuron to grow at a different rate. We first formalize what it means to take a non-uniform trajectory.

**Definition 9** (Non-uniform saturation trajectory) Let  $c(t) : \mathbb{R}^+ \rightarrow \mathbb{R}^n$  where, for all  $1 \leq i, j \leq n$ ,<sup>3</sup>

$$\lim_{t \rightarrow \infty} c_i(t) = \infty \quad (69)$$

$$\lim_{t \rightarrow \infty} \frac{c_i(t)}{c_j(t)} \neq 0. \quad (70)$$

For example, say we want one neuron to saturate at a rate of  $\sqrt{t}$ , and another to saturate at a rate of  $5\sqrt{t}$ . We could represent this non-uniform growth within this framework by setting  $c_1(t) = \sqrt{t}$  and  $c_2(t) = 5\sqrt{t}$ . We can recover the uniformly saturated networks  $\mathcal{F}_u$  by setting each  $c_i(t) = t$ .

**Definition 10** (Non-uniform saturation) For a network  $f(x; \theta)$ , the *non-uniform saturated capacity*  $\mathcal{F}_n$  is the set of functions of  $x$  of the following form, over all possible  $\theta$ :

$$f_n(x; \theta) = \lim_{t \rightarrow \infty} f(x; c(t) \cdot \theta). \quad (71)$$

**Theorem 9**  $\mathcal{F}_u = \mathcal{F}_n$ .

*Proof.* As  $\mathcal{F}_n$  generalizes  $\mathcal{F}_u$ , we know  $\mathcal{F}_u \subseteq \mathcal{F}_n$ . The goal is to show the other direction.

We will define an ordering over every  $c_i$  based on which function is larger asymptotically. For every  $i, j$ , define  $c_i \geq c_j$  iff

$$\lim_{t \rightarrow \infty} \frac{c_i(t)}{c_j(t)} \geq 1. \quad (72)$$

Since  $n$  is finite, a maximum  $c_i$  must exist according to this ordering. Going forward, let  $i$  denote the index of this maximal function. By the definition of non-uniform saturation,  $\lim_{t \rightarrow \infty} c_i(t) = \infty$ . We show how to replace each  $\theta_j$  with  $\theta'_j$  such that

$$\lim_{t \rightarrow \infty} c_j(t) \cdot \theta_j = \lim_{t \rightarrow \infty} c_i(t) \cdot \theta'_j. \quad (73)$$

Consider each index  $j$ . For some constant  $k$ ,  $\lim_{t \rightarrow \infty} \frac{c_j(t)}{c_i(t)} = k$ . We set  $\theta'_j = k\theta_j$ . This implies that

$$\lim_{t \rightarrow \infty} c_i(t) \cdot \theta'_j = \lim_{t \rightarrow \infty} c_i(t) \cdot \frac{c_j(t)}{c_i(t)} \theta_j \quad (74)$$

$$= \lim_{t \rightarrow \infty} c_j(t) \cdot \theta_j. \quad (75)$$

<sup>3</sup>We implicitly assume the following limits exist.



Applying this transformation to every parameter in the network produces a function within the uniform saturated capacity that is equivalent to  $f_n$ , completing the proof.  $\square$

**Corollary 9.1** (Restates Theorem 1) *Let  $\theta(t) \in \mathbb{R}^n$  be the parameter vector of a network  $f(x; \theta(t))$  for  $t$  over the course of training. By  $\theta_i(t)$  we denote a specific scalar parameter. For each  $i, j$ , as  $t \rightarrow \infty$ , assume that  $|\theta_i(t)| \rightarrow \infty$  and  $\theta_i(t)/\theta_j(t)$  converges. Then  $f$  converges to a saturated network as  $t \rightarrow \infty$ .*

*Proof.* Without loss of generality, we can assume  $\theta_i(t)/\theta_j(t) \rightarrow k \neq 0$ . Then Theorem 9 directly applies.  $\square$

## D Accuracy and Norm Growth

We restate the theorems from Section 4, providing full proofs for them. For ease of notation, we write  $f$  for  $f(x; \theta)$ . Assume  $f \neq 0$ .

**Theorem 10** *For a training example  $(x, y)$ , if  $\hat{y} = y$ , then  $\theta^\top \cdot \frac{\partial L}{\partial \theta} < 0$ .*

*Proof.*

$$\theta^\top \cdot \frac{\partial L}{\partial \theta} = \theta^\top \cdot \frac{\partial L}{\partial f} \frac{\partial f}{\partial \theta} \quad (76)$$

$$= (\sigma(f) - y) \cdot \theta^\top \cdot \frac{\partial f}{\partial \theta}. \quad (77)$$

If  $f$  is  $k$ -homogeneous, then  $\theta^\top \cdot \frac{\partial f}{\partial \theta} = kf$  (proved in Lemma 9). Let  $\text{sgn}(\cdot)$  be the sign function.

$$\theta^\top \cdot \frac{\partial L}{\partial \theta} = (\sigma(f) - y) \cdot kf \quad (78)$$

$$= (\sigma(f) - y) \cdot k \text{sgn}(f)|f| \quad (79)$$

$$= -(y - \sigma(f)) \cdot k \text{sgn}(f)|f|. \quad (80)$$

Since  $\hat{y} = y$ , the difference  $y - \sigma(f)$  is asymptotically tightly bounded by a vanishing exponential in  $|f|$ . The sign of the difference is  $\text{sgn}(f)$ . Thus,

$$\theta^\top \cdot \frac{\partial L}{\partial \theta} \leq -\frac{\text{sgn}(f)}{\exp(\Theta(|f|))} \cdot k \text{sgn}(f)|f| \quad (81)$$

$$= -\frac{k|f|}{\exp(\Theta(|f|))}, \quad (82)$$

which is always less than 0 for  $|f| > 0$ .  $\square$

**Theorem 11** *For a training example  $(x, y)$ , if  $\hat{y} \neq y$ , then  $\theta^\top \cdot \frac{\partial L}{\partial \theta} > 0$ .*

*Proof.* We consider two cases depending on the sign of  $f$ .

**Case 1**  $f > 0$ . Then  $\hat{y} = 1$ . Since  $\hat{y} \neq y$ ,  $y = 0$ .

$$\theta^\top \cdot \frac{\partial L}{\partial \theta} = (\sigma(f) - y) \cdot kf \quad (83)$$

$$= (p - 0) \cdot kf \quad (84)$$

for some  $p$  such that  $\frac{1}{2} < p < 1$ . Thus,

$$\theta^\top \cdot \frac{\partial L}{\partial \theta} \geq \frac{1}{2}k|f| \quad (85)$$

$$> 0. \quad (86)$$

**Case 2**  $f < 0$ . Then  $\hat{y} = 0$ . Since  $\hat{y} \neq y$ ,  $y = 1$ .

$$\theta^\top \cdot \frac{\partial L}{\partial \theta} = (\sigma(f) - y) \cdot kf \quad (87)$$

$$= (\sigma(f) - y) \cdot -k|f| \quad (88)$$

$$= (y - \sigma(f)) \cdot k|f| \quad (89)$$

$$= (1 - p) \cdot k|f| \quad (90)$$

for some  $p$  such that  $0 < p < \frac{1}{2}$ . Thus,

$$\theta^\top \cdot \frac{\partial L}{\partial \theta} \geq \left(1 - \frac{1}{2}\right) \cdot k|f| \quad (91)$$

$$\geq \frac{1}{2}k|f| \quad (92)$$

$$> 0. \quad (93)$$

□

Note that, as  $f$  is homogeneous in  $\theta$ ,  $|f|$  is monotonically increasing with  $\|\theta\|$ .

## D.1 Vanishing Step Size

**Theorem 12** *Let  $f : \mathbb{R}^n \rightarrow \mathbb{R}$  be a  $k$ -homogeneous network followed by binary cross-entropy loss. We assume  $\|\nabla f\|$  is bounded over the  $n$ -sphere. Let  $\rho_t = \|\theta_t\|$ . For a training example  $(x, y)$ , if  $\hat{y} = y$ ,*

$$\|\nabla L_{|\theta_t}\| \leq \frac{\mathcal{O}(\rho_t^{k-1})}{\exp(\Omega(\rho_t))}. \quad (94)$$

*Proof.* Reparameterize  $\theta_t = \rho_t \hat{\theta}_t$ , where  $\hat{\theta}_t$  is the normalized parameter vector.

$$\nabla L_{|\theta_t} = (\sigma(f) - y) \nabla f_{|\theta_t} \quad (95)$$

The derivative of a  $k$ -homogeneous function is  $(k-1)$ -homogeneous, so  $\nabla f_{|\theta_t} = \rho_t^{k-1} \nabla f_{|\hat{\theta}_t}$ . Therefore,

$$\nabla L_{|\theta_t} \leq \frac{\nabla L_{|\theta_t}}{\exp(\Omega(\rho_t))} \quad (96)$$

$$= \frac{\rho_t^{k-1}}{\exp(\Omega(\rho_t))} \nabla f_{|\hat{\theta}_t}. \quad (97)$$

We assumed  $\|\nabla f\|$  is bounded over the unit sphere, so  $\|\nabla f_{|\hat{\theta}_t}\|$  is upper bounded by some constant.

$$\|\nabla L_{|\theta_t}\| \leq \frac{\rho_t^{k-1}}{\exp(\Omega(\rho_t))} \|\nabla f_{|\hat{\theta}_t}\| \quad (98)$$

$$\leq \frac{\mathcal{O}(\rho_t^{k-1})}{\exp(\Omega(\rho_t))}. \quad (99)$$

□

## E Other Lemmas

In Theorem 2 and Theorem 3, we rely on the following:

**Lemma 9** *For  $\theta \in \mathbb{R}^n$ , let  $f : \mathbb{R}^n \rightarrow \mathbb{R}^m$  be a function such that  $f(\theta)$  is  $k$ -homogeneous in  $\theta$ . Then,*

$$\nabla f_{|\theta}^\top \cdot \theta = kf(\theta). \quad (100)$$

*Proof.* For all  $c \geq 1$ ,

$$f(c\theta) = c^k f(\theta) \quad (101)$$

$$\frac{d}{dc} f(c\theta) = \frac{d}{dc} c^k f(\theta) \quad (102)$$

$$\nabla f_{|c\theta}^\top \cdot \theta = kc^{k-1} f(\theta). \quad (103)$$

Now, let  $c = 1$ . We get

$$\nabla f_{|\theta}^\top \cdot \theta = kf(\theta). \quad (104)$$

□